THE JOURNAL OF PHYSICAL CHEMISTRY B LETTERS

2006, *110,* 24797−24801
Published on Web 11/15/2006

Side-by-Side Characterization of Electron Tunneling through Monolayers of Isomeric Molecules: A Combined Experimental and Theoretical Study

Jian Liang,[†] Qiang Sun,[†] Annabella Selloni,*[,†] and Giacinto Scoles*[,†,‡]

Department of Chemistry, Princeton University, Princeton, New Jersey 08544, and International School for Advanced Studies and Elettra Synchrotron Laboratory, Trieste, Italy

Received: September 16, 2006; In Final Form: November 2, 2006

We report a new experimental method for measuring relatively small differences in electron tunneling through two distinct monolayers. We place them side by side using scanning probe nanolithography and compare the tunneling currents by conductive probe atomic force microscopy under identical force, voltage, and tip contamination conditions. We demonstrate the validity of our approach by applying it to two isomeric molecules with similar length and functional groups, with only the position of two functional groups, one aromatic and the other aliphatic, being inverted with respect to each other. The relative values of the two tunneling currents, calculated using density functional theory and the Tersoff−Hamann approach, compare very well with the experimental data, providing us with an example of theory vs experiment agreement that is rather uncommon in this field.

Introduction

Scanning probe microscopy (SPM), including scanning tunneling microscopy (STM) and conductive-probe atomic force microscopy (CP-AFM), has been widely used to explore the transport of charge through self-assembled monolayers (SAMs).[1−4] In these experiments the metallic substrate and the conductive probe act as two electrodes. By adding a bias to the electrodes, a current flowing through the nanometer-scale metal/molecule/vacuum/metal junction is obtained. However, controlling the nature of the contact between the SPM tip and the SAM is difficult. In particular, the nanometer scale interactions, the contact area, and the thickness of the vacuum barrier between the tip and the SAM are all quite hard to estimate with good precision. This is likely the reason why the results obtained by different groups in the past 10 years[5−9] are not in agreement with one another. The discrepancies of current-per-molecule values between different CP-AFM data for the same alkanethiol can reach up to 3 orders of magnitude[10] or more and, apparently, cannot be reduced by statistical methods. This is a major issue, not only from the purely experimental point of view but also because it makes the comparison between theory and experiment quite problematic, which is clearly an obstacle to further advances in this field.

In this paper we propose a possible route to significantly improve on this situation. In the new approach, using nanografting (an AFM based nanolithographic method[11]), we fabricate two or more SAMs side by side on the same surface. After nanografting is performed, a new and, at least initially, clean metal-coated tip (at a given bias voltage V with respect to the surface) is scanned above the surface region where adjacent patches of different SAMS are present, so that the current flowing through these monolayers can be recorded in a single experiment. The current map, together with the topography image acquired by the conventional AFM laser-deflection feedback, are simultaneously obtained. This direct comparison minimizes the uncertainties mentioned above by using the same tip and holding the contact force constant.

In this letter, we compare the electron tunneling properties of monolayers made of 4-ethyl-benzenethiol (EtPhSH) and benzeneethanethiol (PhEtSH) self-assembled on a gold (111) surface. These two molecules are isomers and have similar lengths and functional groups, with only the position of the phenyl ring and the aliphatic chain with respect to the S atom and the surface being inverted (Figure 1). Experimentally, a monolayer of PhEtSH is first self-assembled on the gold surface and then a patch of EtPhSH is fabricated into it by dip-pen grafting. In this process, an AFM tip is soaked into a 1 mM EtPhSH/ethanol solution and dried with nitrogen. The tip is then used to shear away the PhEtSH molecules from the gold substrate by applying a relatively large force load. As revealed by a lower (lateral) force scan, a patch of SAM composed of EtPhSH is formed on the exposed gold sites, surrounded by the initial PhEtSH SAM. We note that the source of EtPhSH is the adsorbate on the tip itself.[12] Also, the nanografted SAM is usually as well packed (if not better) as a SAM prepared by self-assembly.[13] Once the grafting procedure is completed, the conductivities of the two SAMs are measured differentially using CP-AFM and next compared with theoretical estimates based on density functional theory (DFT) calculations.

Due to its success in predicting the atomic structures and electronic states of a wide variety of metal surfaces and adsorbed monolayers, DFT currently is the tool of choice for theoretical studies of molecular junctions.[14−17] By means of DFT calcula-

* Corresponding authors. E-mail: aselloni@princeton.edu, gscoles@princeton.edu
[†] Princeton University.
[‡] International School for Advanced Studies and Elettra Synchrotron Laboratory.

10.1021/jp066059v CCC: $33.50

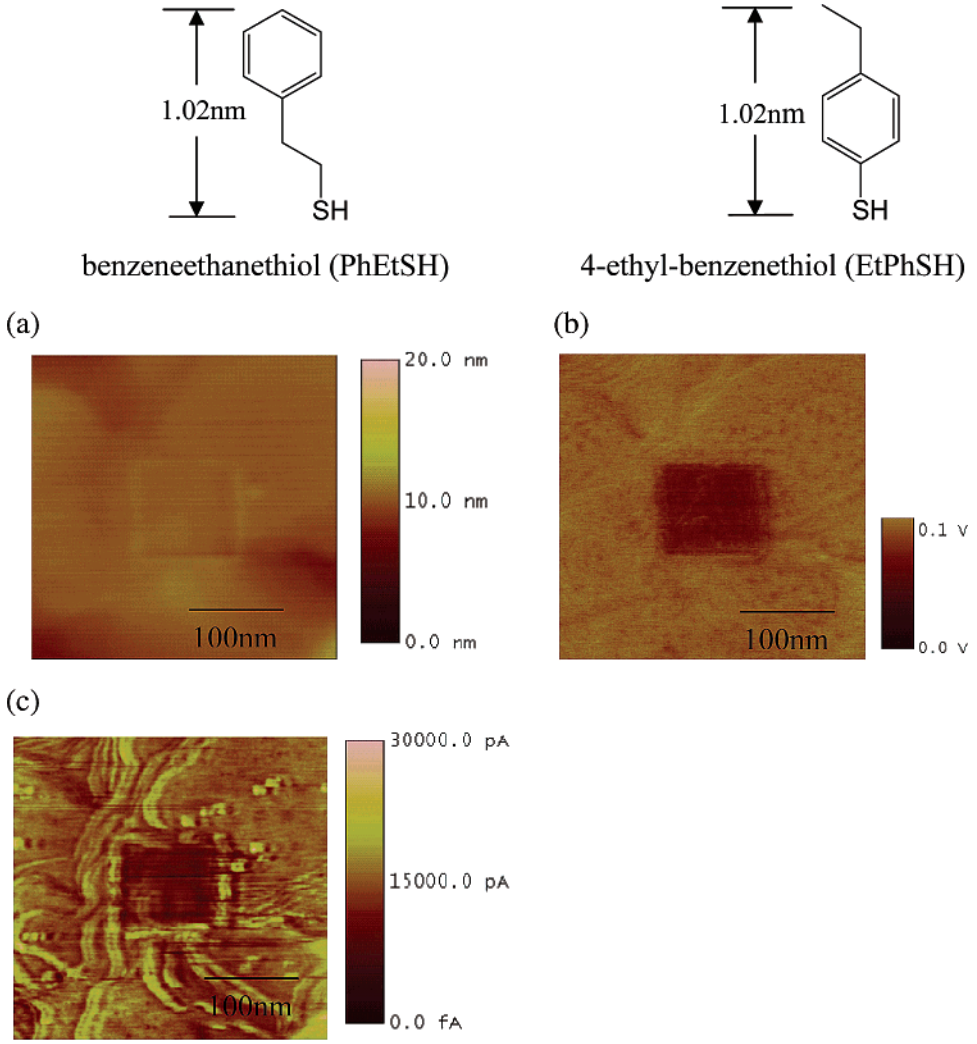

Figure 1. Upper panel: schematic structures of the two molecules. Middle and lower panels: (a) topography; (b) friction; (c) and current images of an EtPhSH patch (100 nm × 100 nm) in the PhEtSH matrix. Panel (c) was obtained at the bias of −300 mV (potential of the tip more negative than the sample).

tions we have investigated the electronic local density of states (LDOS), which plays a crucial role in the tunneling properties. In particular, by studying the spatial dependence of the LDOS at the Fermi energy (E_F) along the molecular wire, we examine the availability of states spanning the entire molecule and therefore capable to contribute to the low bias conductance. As such states do indeed exist for the junctions of interest, we evaluate the current using the Tersoff−Hamann approach,[18] which has been widely applied for many years to interpret STM images and infer surface and adsorbate structures. The resulting I−V curves are found to agree well with the experimental ones. In particular, measured currents are of the order of a few tens nA. Since typical CP-AFM tips have a relatively large radius, ∼10−30 nm, experimental currents actually involve the contributions of hundreds or even thousands of molecules. Thus, the measured tunneling current per molecule should be of the order of 10 pA, consistent with the values predicted by the calculations.

Experimental Section

The Au(111) surface was prepared by thermal evaporation on a heated mica substrate in a vacuum chamber at a background pressure of 1×10^{-7} mbar. After metallization and cooling down to room temperature, the chamber was filled with nitrogen and the sample was taken out and immediately immersed into a 0.1 mM PhEtSH (Sigma-Aldrich, 98% purity)/2-butanol (Sigma-Aldrich, 99.5% purity) solution. A compact monolayer was allowed to form on the Au(111) surface for at least 48 h. Before it was characterized by AFM, the sample was rinsed with absolute ethanol and dried by a gentle flow of nitrogen. As revealed by the AFM, the surface was composed of gold "mesas" with atomically flat tops as large as ∼300 nm in diameter. The flat top was, of course, the region on which we performed nanografting. All the nanolithography and imaging were made using a Digital Instruments MultiMode AFM and a current sensor with a detection limit of ∼50 fA. The dip-pen grafting was performed with Si_3N_4 cantilevers (Veeco Instruments) while the current measurement was carried out with Pt−Ir-coated Si probes (Nanosensors). The applied loads were controlled to be minimal (<0.5 nN) during imaging and current measurement unless otherwise specified, while those for dip-pen grafting were as large as 50 nN.

Results and Discussions

Knowing the thickness of the matrix SAM is not only crucial for judging the conformation of the matrix molecules on the surface, but it is also the prerequisite for determining the height of the grafted molecules. One way to determine the thickness of the SAM is to graft into it a reference molecule with better-known configuration. Alkanethiols are good candidates because

it has been proven by various techniques that the hydrocarbon chain tilts by approximately 30° with respect to the surface normal.[19,20] With this inclination, the vertical height of our reference 1-decanethiol (C10SH) molecule above the gold surface is calculated to be 1.4 nm. From this value and the AFM-measured height difference between C10SH and PhEtSH, we can obtain the thickness of the PhEtSH film. A cross-sectional analysis, which makes direct depth measurements of surface features by producing line profiles on 39 patches, indicates that the C10SH is higher than PhEtSH by 0.5 ± 0.1 nm. Consequently, the thickness of the PhEtSH film is derived to be 0.9 ± 0.1 nm, in good agreement with our DFT calculated height of 9.55 Å for a fully relaxed adsorbed monolayer of standing-up molecules (see below, Figure 4a).

EtPhSH and PhEtSH have similar heights which means that the patch and the matrix can hardly be distinguished in the topographical images (Figure 1a). However, due to their different terminal groups, they show clear contrast in the simultaneously taken friction images (Figure 1b) using lateral force microscopy (LFM). In our experiments, a total of 59 EtPhSH patches were made into the PhEtSH matrix and the statistical height difference was found to be 0.0 ± 0.1 nm. This indicates that the grafted EtPhSH also forms a monolayer in which the molecules are standing up.

Another important issue is the compactness/order of the grafted layer. Recently we compared in-situ the conductivity of a SAM of decanethiols (C10SH) nanografted into a SAM also made of C10SH molecules.[21] In the regions where the surrounding layer was less compact, the measured current showed spikes at the pinholes/defects, but the conductance of the remaining layer (the baseline) was the same as that of the grafted more-compact SAM. Thus, in the following we include only results from the baseline region when discussing the current.

Figure 1c shows the current image of a typical EtPhSH patch in the PhEtSH matrix. It appears that the tunneling current through the grafted EtPhSH patch is smaller (darker image) than through the PhEtSH matrix. At the same time, the height of the patch did not change during and after all the current measurements, indicating that the layers were not desorbed by the relatively low biases.

By averaging the current intensities of a typical EtPhSH patch (denoted as Patch A) under different biases (excluding the edges of the gold steps), the I−V curve for EtPhSH is obtained (see Figure 2a). Similarly, the I−V curve for PhEtSH is obtained by averaging the current intensities of a flat region in the matrix. From Figure 2a, we can see that at every voltage value between −1 V and +1 V, the current through EtPhSH is always smaller than that through PhEtSH. Each data point is the average of three measurements recorded using the same tip at minimal normal force. Although the fluctuations of current for a given molecule in different current maps recorded at the same bias can reach 50%, the order of the conductivity of the two molecules never reversed in any of the measurements.

Figure 2b shows I−V curves obtained on a different EtPhSH patch (named Patch B) and its surrounding matrix, using the same AFM tip but increasing the normal force to 11.7 nN. Note that these curves are smoother than those obtained at minimal force (Figure 2a), probably because of a more stable contact between the surface and the tip. In Figure 2b the current values are also larger by a factor of 2−3 compared to the data in Figure 2a. Tunneling currents decay exponentially with increasing distance. In particular, for gold the current through vacuum is known to change by an order of magnitude when the tunneling

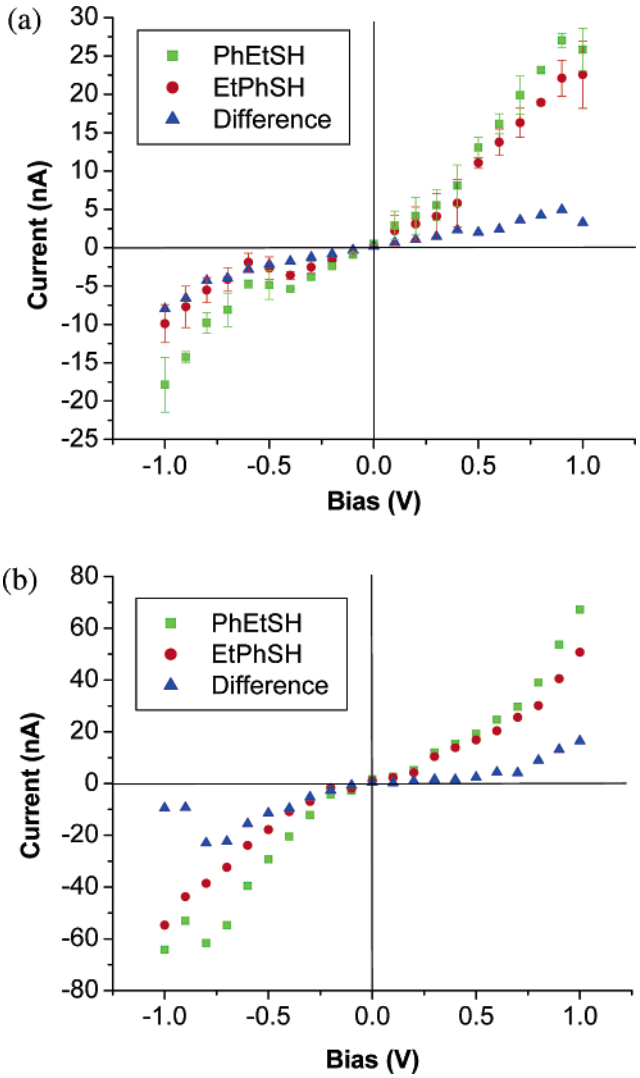

Figure 2. I−V curves derived from different EtPhSH patches in a PhEtSH SAM. (a) Patch A, measured at minimal normal force. Green squares and red circles represent tunneling current through EtPhSH and EtPhSH, respectively; blue triangles represent the difference of the current intensities. (b) Patch B, measured at normal force of 11.7 nN.

distance is changed by 1 Å. Assuming that at the low values of the perpendicular load used in this work the thiol molecules do not change their inclination with respect to the surface, we can deduce that either the tip, under the force of 11.7 nN, reduces the vacuum gap by ∼0.5 Å or that the electrons tunnel through an area of contact that has become a factor of 2 to 3 larger. A combination of the two effects is also possible.

To rationalize our experimental observations, we performed DFT calculations (see ref 15 for details), in which we modeled the substrate/molecule/vacuum/tip junction using a periodic geometry consisting of molecular monolayers sandwiched between slabs of four Au(111) layers. The molecules are chemisorbed through S−Au bonds on one Au(111) surface, representing the substrate, and form a periodic $(\sqrt{3}\times\sqrt{3})$ *R*30 superlattice relative to the gold (1×1) surface. A vacuum gap is present between the molecular terminal groups and the successive Au slab, representing the "tip".[15] A planar surface is a reasonable model for tips with radii of curvature (r_C) much larger than the lateral dimensions of the probed molecule(s), as it is the case for the tips used for AFM measurements, which typically have $r_C \sim 10-30$ nm.

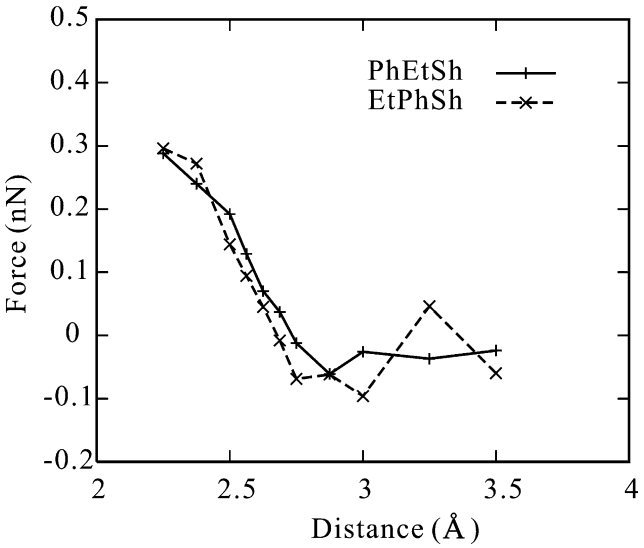

Figure 3. Computed normal force exerted by a molecule on the "tip" as a function of the molecule−tip distance (see text for details).

As a first step, it is important to investigate the relationship between applied force and tip-molecule distance, so as to make sure that the observed differences in the I−V characteristics for EtPhSH and PhEtSH (Figure 2) are actually related to the intrinsic properties of the two molecules rather than caused by differences in the tip−molecule distance. To this end, we performed a series of calculations in which the width of the vacuum gap (tip−molecule distance, d_z) was progressively reduced from 4 to 2.2 Å, while the total system (Au slab plus adsorbed molecular monolayer) was kept in the optimized configuration obtained with $d_z = 4$ Å. For each new value of d_z, the normal force acting on the "tip" (i.e., the Au atoms at the bottom of the slab) as well as the total energy of the slab plus SAM system were monitored. The resulting force (energy)-d_z plots for EtPhSH and PhEtSH show an overall similar behavior (see Figure 3), with the force on the tip becoming repulsive at $d_z \approx 2.7$ Å in both cases. At distances slightly below this value, e.g., d_z= 2.5 Å, the repulsive force due to PhEtSH is actually somewhat larger than that from EtPhSH, 0.20 vs 0.14 nN per Au atom, suggesting that a fixed value of the force in the measurement of the current probably corresponds to a slightly smaller tip−molecule distance for EtPhSH than for PhEtSH, which would affect the measured currents in a way opposite to the observed one. Hence, it seems safe to exclude that the experimental results in Figure 2 are caused by differences in the tip−surface distance. Also note that the experimental error bar on the force is 0.5 nN, which approximately corresponds to 10^{-3} nN per molecule. In correspondence to this, the error on the tip−molecule distance that is predicted by our calculations is 10^{-3}Å or less, and therefore negligible.

Turning next to the electronic properties, we consider the LDOS

$$\rho(\mathbf{r},E) = \Sigma_i |\psi_i(\mathbf{r})|^2 \, \delta(E_i - E) \qquad (1)$$

where ψ_i and E_i are the one-electron (Kohn−Sham) eigenfunctions and eigenvalues. The LDOS at E_F, $\rho(\mathbf{r},E_F)$ for the monolayers formed by EtPhSH and PhEtSH are shown in Figure 4a. It is evident that the LDOS in the conjugated phenyl rings is always higher than in the aliphatic chains. In particular, the LDOS at the terminal group is considerably higher for PhEtSH than for EtPhSH. This difference is further illustrated in Figure

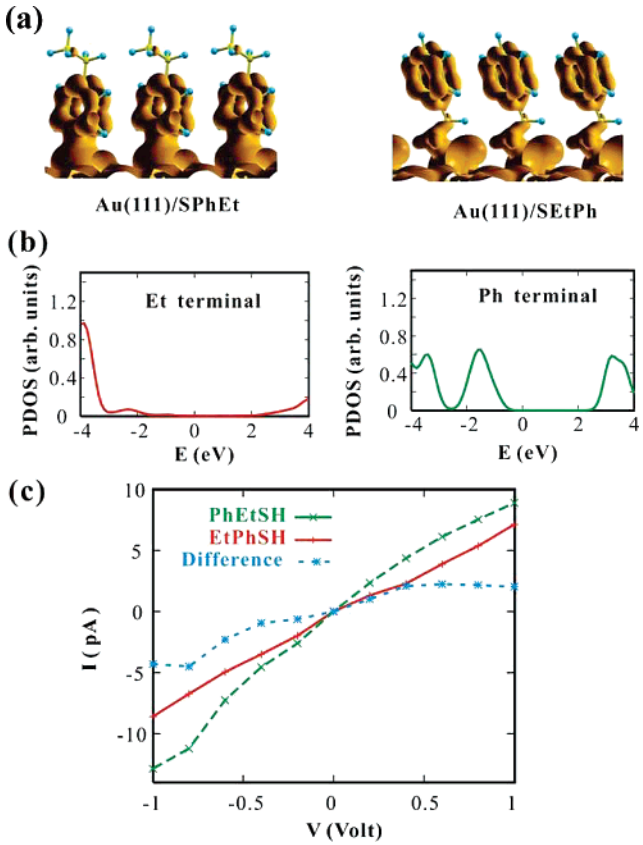

Figure 4. (a) Isosurfaces of constant LDOS at E_F, $\rho(\mathbf{r}, E_F) = 0.01$ a.u, for the two isomeric molecules. (b) Energy dependence of the PDOS at the terminal groups; the zero of the energy scale is set at the Fermi energy E_F. (c) Calculated I−V curves, obtained using eq 2, with $z_0 \sim 1.5$ Å above the molecular terminal.

4b, which shows the projected density of states (PDOS) onto the terminal groups of the two molecules. The PDOS for the Ph endgroup is more structured and larger within a few eV around E_F, due to the fact that the molecular HOMO and LUMO states are largely localized in the phenyl ring.

In spite of the difference in their LDOS, both molecules clearly exhibit states extending throughout the molecule in a range of energies around E_F. This implies that at these energies the minimum of the LDOS for the substrate/molecule/vacuum/tip junction (which represents the "bottleneck" for the tunneling probability) is in the vacuum region between the surface/adsorbate system and the tip, not inside the molecule. We propose that in such a situation (typically found in rather short molecules where the tunneling probability for a valence electron located on the topmost group of atoms to return to the metal is larger than that of tunneling through the vacuum gap) a simple approach, that is Tersoff−Hamann's (TH) theory[18] of the STM, can be used to qualitatively describe the tunneling current. This approximately holds also for cases where the current is measured using a small (non-deforming) applied force, as in Figure 2b, because the tip−molecule contact, which is purely mechanical, still involves a small vacuum gap with no chemical bond formation.

According to TH theory, which is based on the perturbation approach by Bardeen,[22] in the limit of small voltage (V) and temperature the tunneling current from a metallic surface to a spherical tip with radius R and center at $\mathbf{r}_o$ in the vacuum gap is simply proportional to $e\pi R^2 V\rho_S(\mathbf{r}_o,E_F)$, where $\rho_S(\mathbf{r}_o,E_F)$ is the LDOS of the surface at E_F in the absence of the tip electrode. Extending the TH theory to describe finite (but still small relative to the sample workfunction) voltages, V, and assuming that the

tip area is much larger than the area of the surface unit cell (A) over which the tip center is located, we write the tunneling current per unit cell/molecule as

$$I \approx e v_{\text{eff}} \int_A dx\, dy \int_{E_F}^{E_F+eV} dE\, \rho_S(x,y,z_o; E) \qquad (2)$$

where v_{eff} is an effective velocity of the tunneling electrons, and the integral over x and y is carried out in a plane $z = z_o$ well above the molecular apex in the vacuum region. Note that $\rho_S(x,y,z_o; E)$ in eq 2 includes the energy dependence of the transmission probability through the vacuum gap, as the electronic states with higher energy have a slower decay (longer tail) in the vacuum region.[23]

We now apply eq 2 taking $\rho_S(\mathbf{r}, E)$ the LDOS for the Au(111)/molecule system. For these calculations we used a periodic geometry with a rather large vacuum gap of 8.5 Å between the molecule apex and the successive slab, so that there is no interaction between them; in addition, z_o is a point in the vacuum gap ~1.5 Å above the apex of the molecule, where the tails of the charge density of the successive slab are negligible. To estimate v_{eff} in eq 2, we tested two different possibilities, either taking v_{eff} equal to the Fermi velocity for gold or deriving it from the decay constant of $\rho_S(\mathbf{r}, E_F)$ in the vacuum, and found very similar results. The resulting computed tunneling current per molecule for EtPhSH and PhEtSH is reported in Figure 4c. Due to the larger LDOS at the Ph terminal (Figure 4a), we can see that the current is larger for the Ph-terminated case than for the Et-terminated one, in good agreement with the experiment. The values of the computed current per molecule, of the order of a few pA, also suggest that the number of molecules measured in the AFM experiments is $\sim 10^3$, consistent with the typical radius of curvature of an actual tip (10−30 nm).

Conclusions

In conclusion, in this work we have shown that: (i) nanografting can be effectively combined with CP-AFM to distinguish the difference in electron-transfer mediating properties between molecules with subtle structural differences; (ii) these differences can be understood within the simple TH theory of the STM, which appears to describe quite well tunneling through short molecules at low bias. The experimental approach that we propose overcomes many of the difficulties that are encountered in the comparison of results obtained with different setups, which are generally due to the fluctuations of the contact properties. It could be used to explore the electron-transfer properties of surface-bound biomolecules,[24,25] and to study the current−force relationship originated from the deformation of the molecules and/or the position of the tip under different force loads.[26]

Acknowledgment. This work was supported by the NSF (MRSEC Program) through the Princeton Center for Complex Materials (DMR 0213706), and partially supported by DOE under Grant No. DE-FG02-93ER45503. We gratefully acknowledge useful discussions with Simone Piccinin, Roberto Car, Erio Tosatti, Loredana Casalis, Denis Scaini, and the other members of the Elettra/Sissa Nanostructures Laboratory.

References and Notes

(1) Andres, R. P.; Bein, T.; Dorogi, M.; Feng, S.; Henderson, J. I.; Kubiak, C. P.; Mahoney, W.; Osifchin, R. G.; Reifenberger, R. *Science* **1996**, *272*, 1323.
(2) Klein, D. L.; McEuen, P. L. *Appl. Phys. Lett.* **1995**, *66*, 2478.
(3) Friis, E. P.; Andersen, J. E. T.; Kharkats, Y. I.; Kuznetsov, A. M.; Nichols, R. J.; Zhang, J.-D.; Ulstrup, J. *Proc. Natl. Acad. Sci. U.S.A.* **1999**, *96*, 1379.
(4) Xiao, X.; Xu, B.; Tao, N. J. *Nano Lett.* **2004**, *4*, 267.
(5) Cui, X. D.; Primak, A.; Zarate, X.; Tomfohr, J.; Sankey, O. F.; Moore, A. L.; Moore, T. A.; Gust, D.; Harris, G.; Lindsay, S. M. *Science* **2001**, *294*, 571.
(6) Wold, D. J.; Frisbie, C. D. *J. Am. Chem. Soc.* **2001**, *123*, 5549.
(7) Ishida, T.; Mizutani, W.; Aya, Y.; Ogiso, H.; Sasaki, S.; Tokumoto, J. *J. Phys. Chem. B* **2002**, *106*, 5886.
(8) Weiss, P. S.; Bumm, L. A.; Dunbar, T. D.; Burgin, T. P.; Tour, J. M.; Allara, D. L. *Ann. N. Y. Acad. Sci.* **1998**, *852*, 145.
(9) Son, K. A.; Kim, H. I.; Houston, J. E. *Phys. Rev. Lett.* **2001**, *86*, 5357.
(10) Salomon, A.; Cahen, D.; Lindsay, S.; Tomfohr, J.; Engelkes, V. B.; Frisbie, C. D. *Adv. Mater.* **2003**, *15*, 1881.
(11) Amro, N. A.; Xu, S.; Liu, G.-y. *Langmuir* **2000**, *16*, 3006.
(12) Liu, G.-y.; Xu, S.; Qian, Y. *Acc. Chem. Res.* **2000**, *33*, 457.
(13) Xu, S.; Liu, G.-y. *Langmuir* **1997**, *12*, 127.
(14) Nitzan, A.; Ratner, M. A. *Science* **2003**, *300*, 1384.
(15) Piccinin, S.; Selloni, A.; Scandolo, S.; Car, R.; Scoles, G. *J. Chem. Phys.* **2003**, *119*, 6729. Sun, Q.; Selloni, A.; Scoles, G. *J. Phys. Chem. B* **2006**, *110*, 3493.
(16) Xue, Y.; Datta, S.; Ratner, M. A. *J. Chem. Phys.* **2001**, *115*, 4292.
(17) Tomfohr, J. K.; Sankey, O. F. *Phys. Rev. B* **2002**, *65*, 245105.
(18) Tersoff, J.; Hamann, D. R. *Phys. Rev. Lett.* **1983**, *50*, 1998.
(19) Ulman, A. *Chem. Rev.* **1996**, *96*, 1533.
(20) Love, J. C.; Estroff, L. A.; Kriebel, J. K.; Nuzzo, R. G.; Whitesides, G. M. *Chem. Rev.* **2005**, *105*, 1103.
(21) Scaini, D.; Liang, J.; Casalis, L.; Scoles, G., to be published.
(22) Bardeen, J. *Phys. Rev. Lett.* **1962**, *9*, 147.
(23) Datta, S. *Electronic Transport in Mesoscopic Systems*; Cambridge University Press: Cambridge, 1995.
(24) Case, M. A.; McLendon, G. L.; Hu, Y.; Vanderlick, T. K.; Scoles, G. *Nano Lett.* **2003**, *3*, 425.
(25) Hu, Y.; Das, A.; Hecht, M. H.; Scoles, G. *Langmuir* **2005**, *21*, 9103.
(26) Houston, J. E.; Doelling, C. M.; Vanderlick, T. K.; Hu, Y.; Scoles, G.; Wenzl, I.; Lee, T. R. *Langmuir* **2005**, *21*, 3926.